Single-molecule optics

Article *in* Annual Review of Physical Chemistry · February 2004

DOI: 10.1146/annurev.physchem.54.011002.103816 · Source: PubMed

CITATIONS
231

READS
635

2 authors, including:

Michel Orrit
Leiden University
266 PUBLICATIONS **14,497** CITATIONS

SEE PROFILE

Ann. Rev. Phys. Chem. 2004. 55:585–611
doi: 10.1146/annurev.physchem.54.011002.103816

First published online as a Review in Advance on February 10, 2004

SINGLE-MOLECULE OPTICS

Florian Kulzer and Michel Orrit
Molecular Nano-Optics and Spins (MoNOS), Huygens Laboratory, University of Leiden, 2333 CA Leiden, The Netherlands; email: orrit@molphys.leidenuniv.nl

Key Words single-molecule spectroscopy, microscopy, nano-optics, fluorescence resonance energy transfer (FRET), excitons

■ **Abstract** We review recent developments in single-molecule spectroscopy and microscopy. New optical methods provide access to the absorption, emission, or excitation spectra of single nano-objects and can determine either the positions of these objects with subwavelength accuracy or the full three-dimensional orientation of their transition dipole moments. Recent work aims at using single molecules as nanoparts or nanoelements in a variety of molecular-scale devices, from triggered sources of single photons to single-molecular switches. A prominent new direction explores the various interactions between molecules within individual multichromophoric systems obtained by chemical synthesis. These systems are the models for natural self-assembled systems such as the light-harvesting proteins of bacteria and green plants, which are currently studied on a single-molecule basis. Another important class of multichromophoric systems are conjugated polymers. The combination of microscopy with time- and frequency-resolved spectroscopy is opening a wide field of new and exciting applications to individual nano-objects.

1. INTRODUCTION

In less than 15 years, single-molecule spectroscopy has evolved from a specialized variety of optical spectroscopy at low temperatures into a versatile tool used to address a broad range of questions in physics, chemistry, biology, and materials science. It started in 1989 with the experiments of Kador & Moerner (1), who detected the absorption signal of an individual dye molecule embedded in a solid matrix at liquid helium temperatures. Soon after that, Orrit et al. (2) introduced single-molecule spectroscopy by means of fluorescence excitation, a more straightforward technique that yielded better signal-to-noise ratios than the absorption method did. Both these approaches rely on spectral selection of narrow zero-phonon lines and, hence, require a sample at cryogenic temperatures. A few years later, Wild and coworkers (3) demonstrated the feasibility of far-field single-molecule microscopy at low temperatures, which can isolate the chromophores spatially in a suitably diluted sample.

Room-temperature investigations of individual chromophores were first conducted by Betzig and coworkers (4, 5), Keller and colleagues (6), and Xie et al. (7), who all used near-field optics to achieve subdiffraction-limit excitation volumes, thus reducing the background noise. Prior investigations of fluorophores diffusing in solution (8, 9) already suggested that detecting immobilized single fluorophores by far-field confocal microscopy should be possible. This was first realized by Trautman et al. (10, 11) and Xie and coworkers (12, 13). Since then, far-field microscopy of individual fluorophores has become an important technique in many fields of science. Wide-field microscopy with total internal reflection (TIR) excitation, as introduced by the Yanagida group (14) and Dickson et al. (15), has become especially important for the study of biological samples.

A number of reviews and books have appeared in recent years (16–23). Most of them consider experiments at low (16, 22) or room temperature (17–19, 21) separately. Plakhotnik et al. (16) provide the last review for single-molecule experiments at low temperatures. They introduce the photophysical properties of organic dye molecules and the crucial concepts of cross section and signal-to-background ratios. The experiments they review include external field effects, dispersed fluorescence spectra, various correlation effects and the dynamical Stark effect, spectral jumps, and two-photon excitation of single molecules. The review by Nie et al. (19) mainly deals with single molecules in solution, a domain that does not overlap the one we review here. The article by Xie & Trautman (17) reviews experiments on immobilized single molecules at room temperature. After describing the optical setups and basic concepts of molecular photophysics and photochemistry, they review experiments on spectral fluctuations, spatial diffusion, conformational changes and fluorescence resonance energy transfer (FRET), and enzymatic kinetics, with a special mention of surface-enhanced Raman scattering (SERS) on single molecules.

The basic concepts and methods of single-molecule microscopy and spectroscopy have not significantly changed in the past five to six years. Here we do not repeat the descriptions of earlier reviews, which remain largely valid. However, in the past few years, the field has expanded and developed considerably. In Section 2 we discuss some methodological developments before describing applications that are relevant for a broad range of systems and phenomena. Section 3 details the uses of single molecules in the broader context of nanoscience, either as parts of small devices (nanoparts) or as probes for processes on nanometer scales (nanoprobes). Section 4 deals with the new phenomena and horizons opened by interactions between single molecules.

2. METHODOLOGICAL DEVELOPMENTS

2.1. Absorption Spectroscopy and Microscopy

The first optical detection of a single molecule (1) involved the measurement of a weak absorption signal. Because the absorption cross section of a molecule is at least two or three orders of magnitude smaller than the section of a focused

laser beam, this absorption signal is very weak and difficult to detect against the shot noise of the unabsorbed photons. Fluorescence, on the other hand, is a low-background signal, which provides much better signal-to-background and hence signal-to-noise ratios (2). Although fluorescence is by far the more convenient and widely used method today, detection of single molecules via their absorption can present a number of advantages. This method would make it possible to study many poorly emitting dyes, and more importantly, it would remove the need for sophisticated optics to eliminate chromatic aberrations and to collect fluorescence over a wide numerical aperture. These attractive features are fuelling efforts by several groups to detect more efficiently the optical absorption of single nano-objects, with the ultimate goal of detecting a single molecule at room temperature. In the past few years, renewed attempts to obtain single-molecule signals not relying on fluorescence have been made.

First, with a simplified version of the original modulated absorption method, Kador et al. (24) have obtained high signal-to-noise ratios for a single molecule, with a lock-in detection of the transmitted beam and a high-frequency modulation of the optical frequency of the single-molecule line at helium temperature. While the signal was much improved compared with that obtained in 1989, this improvement is mainly attributable both to better photophysical parameters of the guest molecule chosen (namely, terrylene, which has a much higher saturation intensity than pentacene does) and to the tremendous progress in the optical design and parts since the time of the early experiments. Even for this low-temperature experiment, however, the signal-to-noise ratio is still much higher with fluorescence detection. For a room-temperature experiment, for which the molecular cross section is reduced by five to six orders of magnitude, the absorption experiment becomes impossible, or at least exceedingly difficult in a far-field geometry. A simple order-of-magnitude calculation shows that saturation and bleaching would severely limit the detectability of the absorption signal of a single molecule against photon noise. For example, in theory, detecting a molecule with a very short lifetime and no bottleneck state by using a highly focused beam and an accumulation time of one second should be barely possible. Some groups are trying to increase the ratio of the molecule's cross section to the beam area by using the subwavelength aperture of a near-field optical microscope. Although the situation can be improved by two to four orders of magnitude, this ratio is still lower than one ten-thousandth at room temperature, and the experiment is difficult even with near-field optics. No conclusive results have been published yet.

Second, Plakhotnik et al. (25, 26) proposed an original detection method. Besides fluorescence, a single molecule elastically scatters light from the exciting laser via its zero-phonon line. The scattered wave can interfere with the incoming wave since the two are coherent. This interference can only be destructive[1] and leads to the absorption signal. In a prior experiment of (25), the scattered amplitude

[1]The relation between the absorption cross section and the forward-scattered amplitude is given by the optical theorem in scattering theory [see (26a)].

interfered with a reflection on the sample surface. The scattered wave has a phase difference with the reflected wave because of the path difference which results from the fact that the scattering molecule does not sit directly at the surface. The phase of the scattered wave also changes as the frequency of the exciting laser is swept through the molecular resonance. Therefore, the interference structure as a function of frequency can be destructive or constructive, causing absorption-like or dispersion-like profiles. This interferometric signature of single molecules is, however, a weaker effect than absorption is for the following two reasons: The optical wave fronts of scattered and reflected beams are not perfectly matched geometrically, and only a small part of the absorbed light (and of the fluorescence light) contributes to coherent scattering. This small part is made up of the photons re-emitted by the elastic component of the zero-phonon line of the 0-0 transition. At room temperature, because of very fast dephasing, this fraction becomes extremely small with respect to fluorescence, similar to the absorption cross section.[2] In addition, the huge broadening of the resonance at room temperature makes a spectroscopic detection of this interferometric signature completely impractical.

Third, a difficulty in detecting absorption is that, by looking at the transmitted beam only, absorption cannot be distinguished from scattering by defects or dust, or for that matter, from any other light-loss process. To detect absorption, one must thus search for absorption-induced signals other than the missing intensity of the transmitted beam, for example, heat dissipation, which leads to a temperature increase around the absorbing object. Photothermal methods have been developed to detect and measure slight temperature changes by purely optical means. Tokeshi et al. (27) used the thermal lens effect produced by light absorption in a solution to detect less than one dye molecule, on average, in the focus. However, because the integration time (several seconds) was much longer than the diffusion time of a molecule in the focus, thousands of individual molecules were necessary to generate the signal, although less than one molecule, on average, was present in the focus at any given time. This detection method is therefore comparable to fluorescence correlation spectroscopy (FCS), where the accumulation of thousands of single-molecule bursts is required for a measurable correlation. But is the photothermal method sensitive enough to detect the absorption signal of a single immobilized molecule within a reasonable accumulation time? A rough calculation shows that a single molecule should be barely detectable against photon noise in a bandwidth of 1 Hz. It is easier to detect a more strongly absorbing object with a higher saturation intensity, for example, a metal nanoparticle. An additional advantage to using such particles is that they are resistant to bleaching. Boyer et al. (28) have detected by optical polarization interferometry the temperature rise around gold nanoparticles. Figure 1 shows an example of such a photothermal image. It was possible to detect particles as small as 2.5 nm in diameter,

[2]The intensity ratio of the elastically scattered light to the fluorescence light is proportional to the ratio of the coherence to population lifetimes, T_2/T_1, i.e., of the order of 10^{-5} at room temperature.

i.e., comparable in size to the fluorescent labels used in molecular biophysics. The use of this photothermal signal is advantageous because metal nanoparticles are the only strongly absorbing objects in many media, including biological ones and this method is therefore totally immune to scattering by cellular structures and organelles (28a). It is also blind to fluorescence by intrinsic cell components and artificial labels.

2.2. Emission Spectroscopy

Fluorescence emission spectra of single molecules were first recorded at liquid helium temperatures for pentacene in *p*-terphenyl by dispersing the single-molecule emission in a spectrograph and imaging it on a liquid-nitrogen-cooled charge-coupled device (CCD) camera (29). Shortly thereafter it was shown for terrylene in polyethylene that some molecules can exhibit emission spectra that are distinctly different from the ensemble spectrum (30); this was attributed to two distinctly different host geometries. A small number of chromophores with significantly deviant spectra were later also observed for pentacene in *p*-terphenyl (31) and terrylene in *p*-terphenyl (32), for which isotopic substitution with ^{13}C was discussed as an alternative explanation. The concept of locally probing structure and dynamics of a host matrix by means of the emission spectra of embedded chromophores is especially attractive when it is implemented in the form of spectral imaging of single molecules, as introduced by Bach et al. (33): The setup can be aligned so that one exposition delivers both the wide-field image of single molecules (zeroth-order diffraction of the spectrograph grating) and their dispersed spectra (first-order diffraction) onto the CCD chip. That way it is possible to explore correlations between spectral features and position for a number of molecules at once.

Emission spectroscopy of single molecules by means of a spectrograph/CCD combination is, of course, also possible in room-temperature microscopy. The first such studies by Trautman and colleagues (10, 11) explored correlations between emission spectra and fluorescence lifetimes for DiI molecules near a PMMA/air interface. Xie et al. (12, 13) observed spontaneous and photoinduced spectral fluctuations of sulphorhodamine 101 in PMMA, which allowed them to make conclusions about the complex energy landscape of the polymer host. Further experiments include the observation of intrinsic conformer jumps of amino-substituted perylenemonoimide derivatives, for which the emission spectrum changes appreciably depending on whether the lone pair of the amino group is in resonance with the chromophore's π-electrons (34), as well as the observation of the self-sensitized photo-oxidation of terrylene at the single-molecule level (35).

It is even possible to measure the coherence length of photons that are emitted by a single nitrogen-vacancy defect in diamonds at 1.6 K (36): A scanning Michelson interferometer can be used to measure the self-interference of photons from the zero-phonon line emission of the color centers. A coherence time that was in good agreement with what one would expect from the spectral line width was found, demonstrating the feasibility of Fourier-transform spectroscopy with single emitters (36).

2.3. Excitation Spectroscopy

Organic molecules emit Stokes-shifted fluorescence. In addition to a resonant emission from the lowest excited singlet state, their fluorescence spectrum shows a number of redshifted lines. This feature, which is nearly absent for semiconductor nanocrystals, makes it possible to record sharp zero-phonon lines in fluorescence excitation spectra, at the cost of rejecting the resonant fluorescence with the exciting-laser light. With single-frequency lasers, excitation spectra display lines as sharp as the excited-state lifetime allows, giving unprecedented detail in subtle molecular interactions and spectral diffusion. This method, however, presents two drawbacks:

1. Only a handful of host-guest systems present the intense and sharp zero-phonon lines matching narrow laser lines.
2. Narrow-band lasers are unwieldy to scan over wide frequency intervals, which makes it difficult to record broadband spectra with a high time-resolution or to investigate large frequency jumps in spectral diffusion.

Two recent papers propose solutions to these problems: Nonn & Plakhotnik (37) proposed recording the vibronic transitions (to the vibrational levels of the excited electronic state) of a single molecule in a fluorescence excitation spectrum. This requires scanning the frequency of the single-mode laser over a range of more than 30 cm^{-1} (which can be done in several minutes with commercially available laser systems). The observed vibronic bandwidths amounted to a few tens of gigahertz (of the order of 1 cm^{-1}) and were free from any inhomogeneous broadening. They are related to fast intramolecular relaxation of vibrational energy. The sample used in that work was not dilute enough to isolate a single molecule in a focal spot so that a few molecules were contributing to a vibronic band. The authors had to use spectral jumps and difference spectra to isolate the signal of a single molecule. In a later publication, Plakhotnik et al. (38) propose an elegant method based on saturation to solve this problem. (Another solution would be to decrease the guest concentration in the sample.) They found a distribution of vibrational frequencies for a small number of molecules, which was correlated to some degree with their electronic transition frequencies.

In more recent work by Kiraz et al. (39), the concentration was low enough to ensure that only one molecule was excited at a time. The molecule was excited at a much higher energy than was used for the 0-0 electronic transition. At this higher energy, the molecule's absorption spectrum is broad and featureless. The excitation gave rise to a zero-phonon line and to redshifted fluorescence lines, and the whole spectrum was recorded at once with a multichannel detector (a CCD camera). Although the spectral resolution is now limited by the spectrograph, this method is advantageous because it does not require that the laser be scanned and it also applies to molecules with broad emission spectra, even if they show no zero-phonon line. The authors recorded spectral diffusion traces similar in shape to those observed in earlier studies of polymers, but spanning 100 times broader

frequency intervals [see Figure 2]. This technique may well be used to study dynamics at low and intermediate temperatures in such systems as proteins or complex materials.

2.4. Single-Molecule Tracking

An important application of single-molecule microscopy is the tracking of labels, i.e., following their position and/or their orientation as a function of time. In the following we review the different techniques that can be used for single-molecule tracking and give the reader an idea about the positional accuracy and temporal resolution that can be achieved.

2.4.1. POSITION TRACKING Spatial tracking of single-molecule labels has yielded a wealth of new insights into various biological and physical processes. As it is generally desirable to achieve a high temporal resolution, the most common approach is to employ wide-field imaging, often in combination with illumination by an evanescent field that is generated by total internal reflection. Even though these far-field techniques are subject to the diffraction limit, they can nevertheless achieve an accuracy in position determination on the order of a few nanometers. This is related to the fact that the centroid of the diffraction-limited spot, which originates from an isolated point source (such as a dye molecule or a subwavelength-sized fluorescent bead), can be determined with an accuracy that is only limited by the signal-to-noise ratio and the mechanical stability of the apparatus during the acquisition time (40, 41). Schmidt et al. (42) showed that a two-dimensional localization accuracy of 30 nm can be achieved with an integration time of 5 ms for single-dye molecules in phospholipid membranes, and Kubitschek et al. (43) reported similar results for green fluorescent protein (GFP) molecules diffusing in viscous solutions or gels. Recent advances in single-molecule position tracking include the real-time imaging by Bräuchle and colleagues (44) of single viruses infecting living cells and the investigations by Yildiz et al. (45) on the mechanism of myosin V movement. The latter study achieved a localization accuracy of 1.5 nm at an imaging rate of 2 Hz and extended the total observation time to approximately 50 s by employing oxygen-scavenging agents. The tracking of single molecules and particles can be extended to three dimensions by a number of approaches, e. g., by using astigmatic detection optics (46) or by exploiting the strong axial gradient of an evanescent field (47).

Here we briefly mention the important technique of fluorescence correlation spectroscopy (FCS) (48), which analyzes the diffusion of fluorescent molecules in dilute solutions by means of the intensity fluctuations that result from their movements relative to the stationary excitation volume. In addition, FCS can be used to address a number of questions about molecular photophysics and conformational dynamics. As an exhaustive description of FCS is beyond the scope of this review, we refer the reader to recent review articles (49, 50).

It is noteworthy that fluorophores can be resolved within the diffraction-limited excitation volume if they can be distinguished by some spectroscopic property (51,

52). This kind of "super resolution" was first demonstrated at low temperatures for single molecules, which could be addressed selectively because of their sharp zero-phonon lines, by van Oijen et al. (53) and Bloeß et al. (54): They managed to determine the relative molecular positions with an accuracy of better than 4 nm in lateral directions and about 100 nm along the optical axis. At room temperature, on the other hand, differences in the emission spectra of particles that can be excited at the same wavelength can be employed. This was shown by Weiss and colleagues (55) for semiconductor nanocrystals and fluorescent beads that could be distinguished and pinpointed with a lateral accuracy of better than 10 nm over micron distances (limited only by the precision of the scan stage).

2.4.2. ORIENTATIONAL IMAGING In addition to being able to pinpoint the location of a single emitter, knowing the orientation of a single molecule's transition dipole moment is desirable. This may be necessary for calculating the distances from measured FRET efficiencies (see Section 4.1) or for using single particles as probes for orientational dynamics. The projection of single-molecule dipole moments onto the object plane can be determined by polarization-modulated excitation, as was demonstrated first at low temperatures (56) and then by near- (7) and far-field (57) microscopy at room temperature. To determine the full three-dimensional orientation of molecular dipoles, it is necessary to get access to their axial component. Near-field excitation automatically provides axial and lateral electric fields, dependent on the position across the subwavelength illumination aperture. Indeed, the first observation by Betzig & Chichester (4) of single chromophores at room temperature by scanning near-field optical microscopy (SNOM) demonstrated how this can be used for three-dimensional orientational mapping. Obtaining three-dimensional orientational information from far-field imaging techniques, on the other hand, makes it possible to study many molecules in parallel. This was first demonstrated at liquid helium temperatures when the out-of-focus images of an immersion mirror objective were used to determine molecular orientation (58). Fourkas (59) showed that a polarization analysis of the fluorescence collected with a high-NA (numerical aperture) objective allows a complete determination of the emitter's orientation. The main problem is then to ensure a sufficient excitation probability for molecules aligned parallel to the optical axis. One way to achieve this is to use TIR excitation with proper direction and polarization of the totally reflected beam (15, 60). Forkey et al. (61) recently demonstrated that the orientation of dye labels can be monitored with a temporal resolution of better than 50 ms by means of a polarization/direction-switching TIR method. This was used to elucidate the "lever arm" mechanism of force generation during myosin V movement. Alternatively, it is also possible to combine polarization-modulated TIR excitation and far-field illumination to determine the axial and lateral components, respectively, of the transition dipole (62).

It is not necessary, however, to use an evanescent field for excitation because the focus of a high-NA objective already contains appreciable axial components. The strength of these components relative to the lateral ones can be greatly enhanced

by using annular (ring-shaped) illumination to study chromophores in the vicinity of a dielectric interface as reported by Hecht and colleagues (63), or by means of radially polarized input beams as demonstrated by Novotny and coworkers (64). Enhancement may also be obtained by using the phase-mask method of Tchénio and coworkers (65), which has the advantage of concentrating the axial field in the central lobe of the focus (65). A high-NA parabolic mirror in combination with size-matched radially or azimuthally polarized doughnut modes also allows one to select longitudinal or transverse polarization components, respectively (66). All these approaches can give rise to a characteristic field distribution in the focus, which, in turn, results in orientation-dependent patterns for molecules in a two-dimensional image. These techniques are thus somewhat similar to orientation determination by near-field microscopy (mentioned above). As with the SNOM method, the images have to be acquired point by point. A recent improvement that allows one to determine the orientation of many molecules at the same time is the introduction of polarization tomography by Prummer et al. (67), who use pre-conditioned beams at the edge of the input aperture of an immersion objective for wide-field illumination of the sample under nearly glancing incidence. Five exposures with illumination from different directions and with different polarizations are enough to reconstruct the orientations of all molecules in the observation area from the relative intensities of their signals in those five images (illustrated for one molecule in Figure 3). This technique promises high bandwidths (up to 200 Hz) and parallel detection (67).

Slightly different possibilities arise when semiconductor quantum dots are used as probes or labels. It was shown, first at low temperatures (68), that CdSe nanocrystals have a twofold degenerate dipole moment of their optical transition. The orientation of such two-dimensional emitters can be determined in a straightforward way from the phase and contrast of their fluorescence signal under in-plane polarization-modulated detection. Bawendi and coworkers (69) recently demonstrated that the two-dimensional emission character of (near-)spherical quantum dots can also be observed at room temperature. It can thus be used to determine their orientation from four polarization-dependent images, which can be acquired simultaneously on four quadrants of a CCD camera used with polarization-dependent beamsplitters in the detection path (69). This new approach is especially interesting because quantum dots are becoming increasingly important as multipurpose biological labels.

3. SINGLE MOLECULES AS NANOELEMENTS

An appealing feature of single molecules is their small size, which makes them relevant to the realm of nanoscience. Single molecules can be considered as components of nanodevices, in which they can fulfill well-defined functions. Many examples illustrating this idea are found in molecular biology. Single molecules may also function as input or output “ports” that transfer information between the macroscopic world and the “nanoworld.” These ideas have spawned several

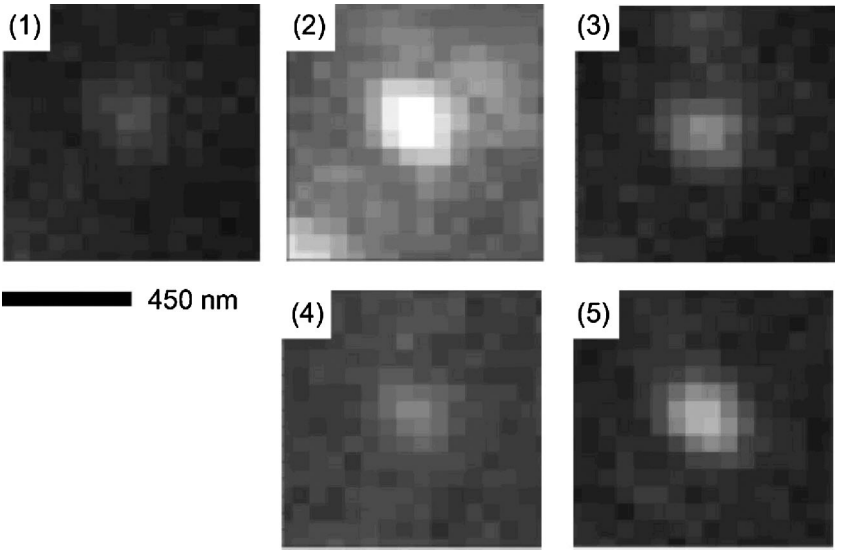

Figure 3 Optical polarization tomography: A series of CCD images of a molecule for different excitation polarizations and directions of incidence. First direction of incidence: (1) p polarization, (2) s polarization, and (3) polarization turned away from p polarization by 45°; second direction of incidence: (4) s polarization and (5) polarization turned by 45°. The relative intensity of these five images yields the full three-dimensional orientation of the molecular transition dipole. Reprinted with permission from Prummer et al. (67). Copyright 2003, American Institute of Physics.

new developments in the past few years, which we briefly review in the following sections.

3.1. Photon Statistics and Single-Photon Sources

The photons emitted by a single nano-object convey much information through their spectrum, direction, or polarization, but a particularly rich source of information is their arrival times. In conventional ensemble measurements, synchronization is required, for example, with a short laser pulse. Single molecules, in contrast, do not require external synchronization to yield time-resolved information: The emission of one photon may act as the start signal for the next one. The time-dependent statistics of fluorescence photons from single nano-objects can thus be exploited even under continuous excitation. One of the early and simplest examples of a time-dependent phenomenon studied in this way is intersystem crossing to the nonemitting triplet state. Transitions to the triplet state interrupt the fluorescence signal, giving rise to on and off times in the stream of detected photons (70). The statistics of the detected photons can be characterized via different ways: the auto-correlation function of the fluorescence intensity, the distribution of delays

between consecutive photons, the distributions of on and off times, the distribution of signal intensities sampled with a given time resolution, or higher-order distributions involving more than two times. A number of theoretical papers (71–79) that investigate the general properties of these statistics and relate them to molecular properties by means of adapted models have appeared in the past few years. Depending on the system under study, different measurement methods can give more or less information. For example, in semiconductor nanocrystals, blinking signals can present long on-times. The large weight of these long periods dominate the correlation function, which is therefore flat and featureless (80), whereas the distributions of on- and off-times (where each long on-time counts only once in a histogram) follow power laws (77). When no long on-times are present, the correlation function follows a power law down to microseconds (74), extending previous measurements of the off-time distribution to shorter times by more than three orders of magnitude.

The distribution of consecutive photons, which can be easily measured with start-stop electronics, usually displays antibunching because a single molecule can never emit two photons simultaneously. Antibunching, a purely quantum feature of light, was demonstrated long ago with atomic beams (81) and trapped ions (82) and was one of the first experiments conducted with single molecules (83). But, antibunching can also be used to manipulate a stream of photons. Better quantum measurements, in particular those for quantum cryptography, could be obtained from a source delivering photons individually, for example, single luminescent nano-objects (molecules, nanocrystals, quantum wells, color centers), which emit individual photons in a triggered or quasiperiodic stream (84–87). The advantage of using nano-objects, with respect to macroscopic devices, is that the uniqueness of the emitted photon is built into the system, as a consequence of the uniqueness of the emitting quantum object. A requirement for this use, however, is that the state of the nano-object must change significantly when one excitation is present. The system then reacts differently to a second excitation, for example, by relaxing it very quickly in a nonradiative way. This is clearly the case for molecules (because of the fast nonradiative relaxation between S_n and S_1, whereas the relaxation from S_1 to S_0 is slow and radiative) and for semiconductor nanocrystals (because of the so-called Auger processes, where free charges relax the exciton efficiently via a nonradiative channel). For self-assembled quantum dots in semiconductor heterostructures (where multiexciton states can emit), low temperatures and spectral filtering are necessary to reject photons emitted by biexciton and higher excited states and to retain only photons emitted by the single-exciton state.

3.2. Structural Dynamics in Glasses

Single molecules can also be used to probe their environment at nanometer scales, which opens applications in molecular biology, materials science, and physical chemistry. Glasses at different conditions have been studied, by doping them with probe molecules. Individual molecules reveal the considerable inhomogeneity and

complexity of glasses at nanometer scales. At low temperatures, much of the macroscopic properties of glasses can be adequately described by two-level systems (TLS). These two-level systems are defects in the glass structure that can assume either of two different conformations and that switch from one to the other by phonon-assisted tunnelling. Although the TLS model was proposed approximately 30 years ago, single-molecule experiments have been the first to provide hard evidence for the physical existence of TLS as individual entities and for their persistence over long periods of time (88). Correlation functions and spectral trails show that TLS are the prevalent degrees of freedom in glasses at low temperature, which account for most glass dynamics. More recent studies have focused on cases showing deviations from the conventional TLS assumptions, giving, for example, evidence for coupling between individual TLS (89, 91). Probe molecules have also been studied in glasses at higher temperatures. Deschenes et al. (92) investigated rotational diffusion dynamics close to the glass transition temperature and showed the large dispersion of diffusion parameters from molecule to molecule and as a function of time for one molecule, which is the main source of the nonexponential ensemble kinetics. Vallée et al. (93) have used the fluorescence lifetimes of molecules dissolved in polymers to probe local density fluctuations. In a simplified picture, a higher density corresponds to a higher local index of refraction, which in turn corresponds to a higher local-field correction of the molecular transition dipole and therefore to a shorter radiative lifetime. They showed that fluctuations require increasingly fewer concerted rearrangements as the polymer approaches its transition temperature from below.

3.3. Charges and Currents

The previous examples show how molecules can probe structural rearrangements of the surrounding matrix via their spectrum, orientation, or fluorescence lifetime. Structural changes involve the motion of atoms with respect to their equilibrium positions. However, other degrees of freedom, for example, the motion of charge carriers in conductors or semiconductors, can be active in solids. They can influence the optical properties of a probe molecule via the electric field they create or via their polarizability. A first step toward understanding this was the study by Caruge et al. (94) of the effect of an electric current in a semiconductor film on the spectra of single molecules in the vicinity of the film. The experiments were done at low temperature to enhance the sensitivity of the molecular line to electrical changes. Single-molecule lines were found to shift and, in some cases, to broaden under the influence of an applied current. The broadening was attributed to a local heating by hot spots in strongly inhomogeneous conduction channels. The shift appears to have a more subtle origin, which involves selective heating of the carrier gas, while the lattice remains cold. As the polarizability of the carrier gas is modified by heating, the semiconductor's interaction with the molecular dipoles shifts the transition frequency. It should be stressed that the effects measured were several orders of magnitude larger than the well-known Stark effect of the applied

electric field. They were, therefore, mediated by the current in the film and not by the voltage. The application of alternating currents to the semiconductor led to surprising resonance effects at frequencies lower than 1 megahertz and as low as a few kilohertz. The origin of these effects may be related to density waves in the compensated semiconductor, localized by the disorder of its grainy structure. More work, better-defined samples, and different sample geometries are required to clarify the origins of these slow dynamical effects.

3.4. Optical Switching

So far, we have mainly described the use of single molecules as "passive" nanoelements that can be employed to probe structural dynamics. Now, we demonstrate how single molecules can act as nanoelements that can be switched "actively" between spectroscopically different states, thereby paving the way toward optical manipulation of matter and information on a truly nanoscopic scale.

3.4.1. OPTICAL SWITCHING AT LOW TEMPERATURES The first manifestations of single-molecule optical switching were observed in low-temperature investigations with narrow zero-phonon lines. Basché and colleagues (95, 96) demonstrated that perylene in polyethylene undergoes light-driven, thermally reversible frequency jumps, the single-molecule analogue of nonphotochemical hole burning. Moerner et al. (97) were the first to observe a two-state single-molecule switch for terrylene in a Shpol'skii matrix of hexadecane. Here, the photoproduct absorption frequencies, which differ from one molecule to the next one, can be identified in some cases. However, this nonuniform behavior and the fact that many molecules do not switch makes it hard to formulate an underlying mechanism.

The most promising example of single-molecule optical switching at low temperatures can be found when terrylene is embedded in sublimated crystals of *p*-terphenyl. The so-called X_1 insertion site (98, 32) with its absorption maximum at 580.38 nm shows an interesting optical-switching behavior: These molecules undergo fully reversible light-driven frequency jumps that can be followed over weeks for any given chromophore (99). Moreover, the behavior is excellently reproducible for all molecules from the X_1 site, meaning that the underlying mechanism can be investigated using a combination of spectroscopic techniques. Upon excitation the X_1 chromophores can be brought to the primary photosite XY, which lies 843 GHz toward higher frequencies. Prolonged excitation of the XY photoproduct restores the X_1 original state in most cases (85%), but a secondary photocycle opens with 15% probability and gives access to three additional spectral positions.

The most important experimental evidence about the mechanism of the frequency jumps was obtained from Stark-effect measurements of the original and the XY photoproduct state (100): It was shown that the terrylene guests are nearly centrosymmetric in the X_1 state, yielding a predominantly quadratic response to an external electric field but that their symmetry is reduced when they are brought to the XY site, which shows a stronger linear Stark shift. Moreover, there are, in

fact, two conformations for the primary photoproduct, which, although identical in their absorption wavelength, can be distinguished by the sign of their linear Stark term. This suggests that a phenyl ring flips on either one of two symmetry-equivalent *p*-terphenyl molecules in the immediate vicinity of the terrylene guest (100). Molecular dynamics simulations by Bordat & Brown (101, 102), which were based on optimized models of *p*-terphenyl and terrylene, have corroborated this hypothesis, and they provide a consistent picture of all terrylene insertion sites, their different photostability (by simulated annealing), and the nature of most of the X_1 photoproducts. An extended model explained the unusually large quadratic coefficients with the existence of a two-level tunnel state in the X_1 configuration (103). The sum of these experimental and theoretical efforts yields a uniquely detailed scenario for light-induced host/guest dynamics at low temperatures and the mechanism of nonphotochemical hole-burning at the single-molecule level.

3.4.2. OPTICAL SWITCHING AT ROOM TEMPERATURE For applications in high-density optical data storage and signal processing, single-molecule switches should preferably operate at room temperature. First steps in this direction were taken with investigations on individual green fluorescent protein (GFP) molecules. A number of GFP mutants can be observed at the single-molecule level by using TIR excitation (104, 105), epi-illumination confocal (106) and wide-field microscopy (43), as well as SNOM (117). In all instances, pronounced on/off dynamics were observed, which are attributed to a photochemical proton transfer reaction converting the fluorescent anionic form of the protein into the neutral one, which does not fluoresce. For two mutants, the excitation of the protein in its dark state, which absorbs at shorter wavelengths, was used to stimulate the conversion back into the anionic form and thus "switch on" the fluorescence again (104). Investigations of another GFP mutant by FCS with two-color excitation have revealed a similar effect of short-wavelength excitation and could be used to fully explore the pertinent photophysical parameters (108), leading to a two-color excitation scheme for increased signal strength of immobilized individual GFP molecules (109). It should be noted, however, that photobleaching is a particularly severe problem for single-molecule investigations of GFP (and other autofluorescent proteins).

There have been nice examples of single-molecule switches that were specifically designed and synthesized to perform this function. Hugel et al. (110) realized an opto-mechanical switching cycle with polymer strands comprised of approximately 50 azobenzene units. The azobenzene motif can be converted from an extended *trans* to a shortened *cis* configuration (and vice versa) by illumination with blue (near-UV) light. Single strands of this polymer, which had a length of roughly 90 nm, were suspended between a glass substrate and a functionalized atomic force microscopy (AFM) cantilever. Optical excitation by TIR then allowed the strands to switch between the extended and the shortened configuration of the polymer; the TIR illumination was chosen to avoid thermomechanical perturbations due to absorption of the optical stimulus by the cantilever. The changed length and compliance caused by the optical switching can easily be seen in force/extension

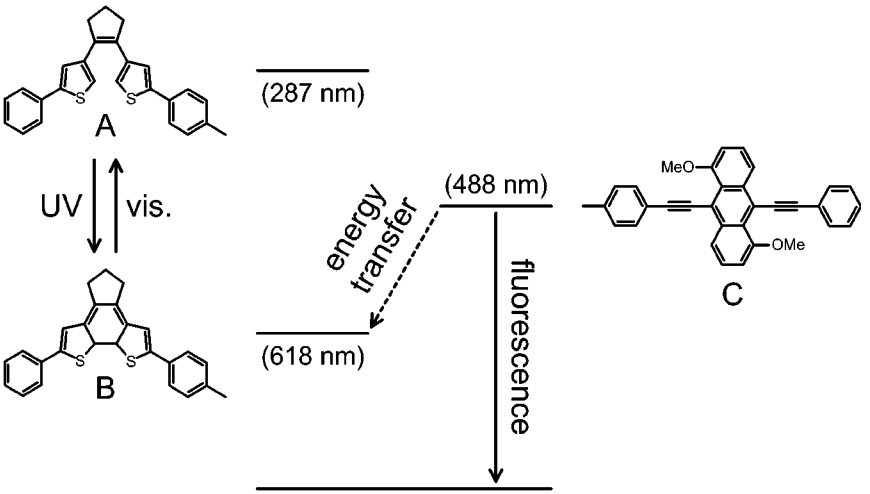

Figure 4 A single-molecule optical switch consisting of a photochromic quencher (*A*, *B*) and a chromophore subunit (*C*), which are linked by an adamantyl spacer (not shown). The open-ring form (*A*) cannot act as an acceptor for the excited state energy of the chromophore subunit (*C*), which then relaxes (mainly) by fluorescing (*solid arrow*). UV irradiation produces the closed-ring form (*B*) that efficiently quenches the fluorescence of the chromophore (*dashed arrow*). The diagram has been simplified by omitting all substituents of the switchable quencher. Adapted from Reference 111.

curves, and it is feasible to optically contract the *trans* form against a force load (110). This made possible the realization of an optomechanical single-molecule "machine" that can operate in a cyclic way to convert optical energy into mechanical work: Repeated optically induced contraction (*trans* → *cis*) under high load (200 pN) is always followed by optically induced extension (*cis* → *trans*) under reduced load (100 pN).

A purely optical single-molecule switch was realized by linking a fluorescent anthracene derivative to a photochromic quencher through a rigid adamantyl spacer (111) (see Figure 4 for the schematic structures). The quencher, a diarylethene derivative, undergoes reversible photoisomerization from an open-ring to a closed-ring form. The open-ring form, which absorbs in the UV region (287 nm), cannot quench the fluorescence of the anthracene chromophore whose electronically excited state lies at a lower energy (488 nm). However, a few seconds of weak UV illumination bring the quencher into its closed-ring form, which has its first optical transition around 618 nm. In this case, efficient energy transfer (99.9%) from the chromophore is possible, which effectively "turns off" its fluorescence. Irie et al. (111) observed the entire process in a polymer film at the single-molecule level by using confocal microscopy: UV irradiation switches off the emission of the individual fluorophores, and illumination with a 488-nm laser light restores the

fluorescent state as the constant energy transfer from the chromophore eventually returns the quencher to its open-ring form. The low-quantum efficiency of this photocycloreversion (8.0×10^{-5}) allows one to discriminate between just detecting single molecules (testing if a given one is currently "on" or "off") and actively switching them "on" again, even though light of the same wavelength is used for both tasks. This example shows how optical functionalities can be integrated at the molecular level by clever chemical design.

4. INTERACTING SINGLE MOLECULES

4.1. Interaction Mechanisms

Interactions between a fluorophore and molecules of the matrix or solvent are responsible for changes in molecular properties, for example, the solvent shift, i.e., the (usually red) shift of the electronic excitation energy when the molecule goes from gas phase to solution. Variations in the solvent shift are responsible for the spectral diffusion of single molecules following molecular rearrangements in their environment. The solvent molecules causing the solvent shift remain in their ground state. We now consider interactions between two (or more) single molecules, both of which can be electronically excited. Besides the electrostatic and van der Waals interactions causing solvent shifts, which are still present, new types of interaction can now arise, leading to an exchange of excitation between the molecules. This exchange may proceed via two essentially different mechanisms.

The first mechanism is a Coulomb interaction. This mechanism can be seen as the exchange of a virtual photon, which is emitted by the excited molecule *A* and absorbed by the ground-state molecule *B*. Usually, the transitions involved are dipole allowed, and this dipole-dipole interaction decays as the inverse-cube of the distance between molecules *A* and *B*.

The second mechanism is a double-electron exchange in which one electron hops from the excited orbital (LUMO) of molecule *A* to an empty excited orbital (LUMO) of molecule *B*, while another electron hops from the ground-state orbital (HOMO) of molecule *B* to the lower orbital (HOMO) of molecule *A* to ensure neutrality. Because electron exchanges require the overlap of orbitals between the two molecules, this interaction decreases exponentially with distance, much faster than the Coulomb interaction. This mechanism must be considered only for molecules in close contact or for optically forbidden transitions.

The motion of electronic excitation between two molecules can take different forms. For fluorescence resonance energy transfer (FRET), the energy transfer from a higher-energy molecule (the donor) to a lower-energy one (the acceptor) can be irreversible if their excited-state-energy difference is larger than the thermal energy. For lower energy differences or for higher temperatures, the excitation can hop back and forth between the two molecules. Such exciton hopping is common in molecular crystals and aggregates at room temperature. Finally, the excitation can be shared coherently between two resonant or near-resonant molecules if

the interaction is larger than or comparable to their excitation energy difference. One then has a coherent exciton with a well-defined phase relation between the excitations on the two molecules. These three cases have been observed in recent years with single molecules (see below).

4.2. Dipole-Dipole Pairs

The FRET rate, given by Fermi's golden rule, is proportional to the square of the interaction and therefore decreases as the inverse sixth power of the donor-acceptor distance. Typical values of the Förster radius, the distance at which the transfer rate equals the donor's fluorescence rate, range from 2 to 10 nm. At the usual concentration of single-molecule experiments, the probability of finding a donor and an acceptor within the Förster radius is very low. Therefore, donor and acceptor have to be part of the same molecular system. Single-pair FRET was first demonstrated by Weiss and coworkers (112) with short DNA strands carrying one donor and one acceptor. These experiments have developed into a method to investigate the structure and dynamics of biomolecules via FRET efficiency, directly related to the distance between donor and acceptor (112, 113). In homodimers, molecules containing two copies of the same fluorophore, one of them often plays the role of an acceptor when it is in its singlet (114) or triplet (115) excited state because the gap between consecutive (excited) electronic levels usually decreases for higher states. Because fluorescence from higher excited states is often weak or absent (this fact, arising also from the decreasing gap between levels, is known as Kasha's rule), an excited molecule acts as a quencher for the fluorescence of its neighbors. In polychromophoric molecules, in dendrimers, or polymers, several chromophores present nearly the same excitation energy. At room temperature, excitons hop from site to site according to thermal fluctuations and fluctuations in local site energy. A consequence of this hopping is that excitons can travel long distances in large structures and get trapped at defects or they can relax nonradiatively at excited molecules. Therefore, fluorescence can arise only from one site at a time in a cluster of molecules connected by hopping. This means that fluorescence light from such a system is antibunched (114). Coherent excitons occur in molecular crystals and aggregates or in small assemblies such as bacterial antenna complexes (see Section 4.3). We briefly discuss a dimer with a splitting Δ of excitation energies and an (Coulomb dipole-dipole) interaction V. For large Δ, the exciton states are localized on each molecule and only weakly perturbed by the interaction. For $\Delta = 0$, on the other hand, new eigenstates appear corresponding to in-phase and out-of-phase oscillations of the molecular dipoles with an equal probability density of the excitation on each molecule. The phase relation between the dipoles gives rise not only to new transition frequencies, but also to new strengths and orientations of the transition dipole moments of the dimer, as compared with those of the isolated molecules.

A nice example of a coherent exciton in a single pair of molecules was described by Hettich et al. (116) using two terrylene molecules in a *p*-terphenyl crystal.

They accidentally found two molecules within 10 nm of each other and located them via the Stark effect caused by a metal-coated scanning tip. To observe a coherent exciton over such a large distance and therefore with a comparatively weak interaction V, the splitting Δ has to be very small (a few gigahertz only), which requires a high quality crystal. Because the splitting Δ could not be varied, the interaction could not be demonstrated by following the energy of the eigenstates. By recording excitation spectra of this dimer at increasing laser intensities, these authors found a new line appearing only at high intensities, right in the middle of the two parent lines of the individual molecules or eigenstates [see Figure 5]. This new line arises from simultaneous excitation of the two molecules with two photons with the middle frequency. The new line can appear only if there is an interaction between the two molecules, so it can be considered a signature of the interaction. Hettich et al. (116) considered two interaction mechanisms: the Coulomb dipole-dipole interaction and a "proximity" interaction, which arises from the variation of the solvent shift of molecule *A* when molecule *B* is excited (and vice versa). The excellent agreement of their fits with all experimental spectra enabled the authors to determine all the excitonic parameters in this system. The ability to create and manipulate quantum superpositions of states is a prerequisite for utilizations of quantum mechanics, such as quantum computing. This simple example of a single pair of coupled molecules is a first step in that direction.

4.3. Antenna Complexes

Interesting examples of interacting chromophores can be found in the antenna complexes from the outer membranes of photosynthetic bacteria and plants. These complexes constitute efficient systems to absorb ("harvest") light energy and funnel it toward a reaction center where it is used to effect a charge separation and generate a proton gradient across the membrane. This proton gradient is then used to drive the synthesis of ATP to complete the photosynthetic conversion of radiation into chemically stored energy. Single-molecule studies of various antenna complexes have helped to improve our understanding of the photophysics of this important biological process.

Extensive single-molecule data are available on the light-harvesting 2 (LH2) complex of the photosynthetic purple bacterium *Rhodopseudomonas acidophila*. This complex consists of 27 bacteriochlorophyll a (BChl a) cofactors that are arranged in two substructures, the B800 and the B850 ring [see Figure 6 for a schematic presentation of the arrangement of the BChl a chromophores]. The strength of the dipole-dipole coupling between the different chromophores and the inhomogeneities in the energies of their optical transitions determine the light-harvesting properties of the complex, and single-molecule techniques allow us to address these issues unhampered by ensemble averaging (intercomplex inhomogeneities).

Individual LH2 complexes can be investigated by room temperature confocal microscopy when they are immobilized on charged surfaces such as mica (118):

Bopp et al. found by polarization microscopy that the complexes behave like elliptical absorbers with their degree of eccentricity and the orientation of their principal axes fluctuating in time (119). The difference in dipole-dipole coupling between the B800 and the B500 cofactors and its effects on energy transfer are nicely illustrated by the low-temperature investigations of van Oijen et al. (120): The B800 pigments are weakly coupled; therefore it is possible to observe well-separated fluorescence excitation lines in the B800 band of individual LH2 complexes at 1.2 K. A rotation of the excitation polarization, furthermore, shows that the lines correspond to largely localized excitations with their polarization-dependent intensity reflecting the different orientations of the individual pigment transition dipoles. The B850 band, on the other hand, has to be described in terms of the exciton model. Here the coupling between the BChl a molecules is so strong that it gives rise to excitonic states coherent over the whole ring. These states are sensitive to variation Δ in the transition energies of the B850 chromophores (diagonal disorder) and to variations in the coupling strengths V for different pairs of chromophores (off-diagonal disorder). Low-temperature fluorescence excitation spectra provide direct access to the energy splitting, polarization dependence, and relative oscillator strengths of these excitonic states (121). The distributions of these parameters reflect the disorder in the complexes, and the measured distributions are best explained by assuming an elliptical distortion of the complexes (121, 122), similar to what has been observed at room temperature (see above). Further insight into the question of static versus dynamic disorder could be gained from the temperature-dependent fluctuations in the B850 fluorescence emission of single complexes seen by Tietz et al. (123) and the direct observation by Hofmann et al. (124) of temporal variations in the coupling strength between pigments in the B800 ring of LH2 complexes from *Rhodospirillum molischianum*.

A number of other antenna complexes, including light-harvesting complexes whose high-resolution X-ray structure is not available yet, have also been investigated with single-molecule techniques. Various issues have been addressed: the coupling strength between the chlorophyll chromophores in LHII complexes of green plants (125), the influence of the membrane environment on the geometry of LH1 complexes from purple bacteria (126), the temperature-dependent fluorescence quenching due to thermally activated energy transfer from the chlorophyll pigments to the reaction center in bacterial photosystem I complexes (127), the energy transfer heterogeneities in phycoerythrocyanin monomers (128), and the collective on/off jumps in the fluorescence of the 34 bilin chromophores of B-phycoerythrin (129, 115). Finally, an illustrative example of exciton dynamics, photophysics, and photochemistry in antenna complexes can be found in the investigation of allophycocyanin trimers (130, 131): Changes in the fluorescence lifetime and differences in photostability between continuous wave (CW) and pulsed excitation provide direct insight into two-photon mechanisms of exciton-exciton annihilation that lead to trap formation and photobleaching. Polarization-dependent excitation, furthermore, reveals the successive bleaching of the individual chromophores and its consequences for the exciton states.

In addition to their important biological functions, antenna complexes are the first example of a strongly coupled system of a few chromophores that can be studied individually. Their new photophysical properties (as compared with those of the monomers) illustrate the wealth of novel effects that can be expected or designed in molecular aggregates and assemblies.

4.4. Artificial Antenna Systems

Organic chemistry has made significant progress in the synthesis of multichromophoric molecules that, at least partially, mimic the natural antenna complexes discussed in Section 4.3. An important class of template molecules that can be utilized to link chromophore subunits in reasonably rigid structures are dendritic macromolecules. These dendrimers can be synthesized by adding a controlled number of hyperbranched shells—normally referred to as generations—to a suitable core structure. This approach produces macromolecules that have binding sites for chromophores around their rim. The number of these binding sites increases geometrically with the generation of the dendrimer. (However, the maximum number of generations for a given dendrimer type is limited by steric hinderance.) Below we summarize how single-molecule studies on polyphenylene dendrimers containing peryleneimide (PI) chromophores on their rim illustrate various aspects of the chromophore-chromophore interaction.

Comparison of a second generation (g2) dendrimer (eight PI chromophores) with a model compound—the dendrimer core (g0) with 1 chromophore attached—at the single-molecule level reveals more dynamics and intensity steps in the fluorescence trace of the g2 dendrimer as well as increased dynamics in the emission spectrum (132). Furthermore, successive bleaching of the chromophores in the g2 dendrimers can be seen from changes in the polarization direction of the emitted fluorescence, increasing contrast for polarization-modulated excitation as the number of absorbers decreases, and in correlations between the fluorescence intensity level, the shape of the emission spectrum, and the fluorescence lifetime measured for the same dendrimer at different times (133). The coupling between the chromophores and the resulting energy hopping manifest themselves in the collective on/off blinking behavior, which is probably caused by the formation of a charge-separated trap state that quenches the fluorescence of all chromophores in the macromolecule (115). The observation of antibunching in the fluorescence emission of g1 dendrimers—holding four chromophores that are closer to each other than the ones in g2 and, hence, couple more strongly—illustrates that, even though all chromophores are excited by the laser irradiation, only one of them acts as the active emitter at a given time. All excitation energy is then transferred efficiently to that chromophore (114).

Other demonstrations of chromophore coupling and energy funnelling include (*a*) measurements on a dendrimer with four PI donor molecules on the rim and a terrylenediimide acceptor in the core (134), which show energy transfer and donor/acceptor photobleaching directly in the emission spectrum, and (*b*) low-temperature investigations on a g1 dendrimer, for which frequency selective

excitation of the zero-phonon lines of individual chromophore subunits was demonstrated (135). The level of control that is possible in the synthesis of different multichromophoric dendrimers suggests that more model systems for photophysical studies of energy transfer at the single-molecule level will become accessible.

4.5. Conjugated Polymers

Another important class of multichromophoric macromolecules are conjugated polymers such as poly(*p*-phenylene vinylene) (PPV) and poly(*p*-pyridylene vinylene) (PPyV), which are used in light-emitting devices and other photonics applications. The optical properties of these polymers are best described in terms of localized excitons whose coherence length extends over a few monomer units only. Efficient electronic energy transfer between the different exciton segments of the polymer chain then leads to an emission dominated by a small number of sites, which correspond to minima in the optical band structure. Next we summarize how Barbara and colleagues used single-molecule spectroscopy to visualize directly the effects of these processes and, in combination with simulations, to provide new insights into the factors that influence the conformation of the macromolecules.

Studies on a derivatized PPV-PPyV copolymer with an average length of approximately 20 monomer units, single strands of which were isolated in polystyrene at room temperature, give direct evidence of the strong coupling between the chromophore subunits (136). Discrete single-step photobleaching was observed for all of the hundreds of polymer molecules that were investigated. In contrast, the gradual fading that would be expected if the chromophore subunits bleached independently was never seen. Moreover, the photoblinking behavior that all molecules showed before bleaching was characterized by the occurrence of only a few distinct intensity levels. This behavior can be understood if one assumes that all absorbed energy is efficiently funnelled toward a small number of low-energy sites. Any process that converts such a site into a fluorescence quencher will then effectively "extinguish" all chromophores that are coupled to this particular site. This process is either reversible or irreversible. A two-color excitation technique—based on alternately exciting a polymer molecule in the red and in the blue edge of the absorption band—showed that the fluctuations in the fluorescence intensity were independent of the excitation wavelength and, hence, cannot be caused by spectral shifts of the absorption band (136). The fact that quencher sites are created photochemically was proven by intensity-dependent measurements of the distribution of "on" and "off" times in the photoblinking traces. As expected, the duration of the "on" timescales was inversely proportional to the excitation intensity, whereas the "off" times are independent of it (136). The most likely hypothesis for the mechanism of the fluorescence quenching is light-induced charge separation generating long-lived local charges that promote radiationless relaxation channels for all subsequently generated excitons (137).

The single-molecule studies described above were extended to a longer PPV derivative (MEH-PPV), which, on average, consisted of approximately 1700 monomer units (138). Similar to the derivatized PPV-PPyV (see above),

the MEH-PPV molecules have a limited exciton coherence length (approximately 10–15 monomer units) so that a single polymer strand of this size consists of approximately 140 quasichromophores. Nevertheless, the polymer molecules still exhibit a collective blinking and bleaching behavior with only a few intensity levels in the single-molecule fluorescence time traces (138). The same efficient energy funneling and collective quenching processes happen in the longer polymers as well. The polarization modulation experiments that were conducted (138, 139) using MEH-PPV provided important new information about the shape that the polymer strands assume in the solid matrix (polystyrene or polycarbonate), since the modulation depth is related to the anisotropy of the angular dipole distribution (138, 139). Even though the full three-dimensional polarization anisotropy was not explored—this could have been done with one of the methods described in Section 2.4.2—it was sufficient to compare the observed distribution of modulation depths with the predictions of Monte Carlo simulations (139). Polymer strands with a length of 250 monomer units were modeled as beads on a chain with each bead representing 2.5 repeat units. If no interaction between the beads is taken into account, the simulations predict a random coil configuration for the polymers, whereas for a Lennard-Jones attraction potential, one finds a collapse into a molten globule state (139). If the bond angle distortion energy is added as a harmonic potential around a minimum energy angle of 180°, toroid and rod-like shapes become the dominant species. However, none of the parameter sets described so far could account for the observed modulation anisotropy. Only if tetrahedral defects (sp^3 carbon atoms), which exist in these types of polymers with an overall probability of 1–5%, are added to the simulations is the observed distribution of modulation depths recovered, by predicting defect-coil and defect-toroid configurations (139). A knowledge of the configurations and of how they are influenced by, e.g., the spin coating conditions is important for many aspects of the technical processing of the MEH-PPV polymers.

In addition to the technical implications of the single-molecule studies on MEH-PPV, there are interesting illustrations of photophysics. An improved sample preparation method, which removes oxygen from the polymer films by degassing them in vacuum and subsequently sealing them with a vapor-deposited metal layer (140), allowed for a dramatically better signal-to-noise ratio and a direct demonstration of the energy funneling toward low-energy sites. It was possible to compare emission spectra of the polymer molecule in its unphotolyzed and its (partially) photolyzed state, and the difference spectrum directly shows the narrow and redshifted emission spectrum of the low-energy trap site that is quenched in the photolyzed state (140).

5. CONCLUSION

The field of single-molecule optics has matured considerably in the past five to six years. The unbound enthusiasm of the early days has now given way to a more down-to-earth but sounder approach to many problems, and to a critical appraisal

of when single-molecule methods are preferable and of what new information they can provide. The field has witnessed a dramatic broadening in the range of particles studied, which now includes metal nanoparticles, nanotubes, or color centers in addition to more conventional emitters such as nanocrystals and the organic fluorophores that are the main subject of this review. The molecular systems in which these emitters are integrated now include electronic circuits, glasses close to the transition temperature, and an ever broadening variety of biological constructs and native objects going from labeled proteins to living cells and viruses. This review covers a time span in which researchers conducted several experiments that had previously been dreams. The following are but a few examples of these: the determination in parallel of the full three-dimensional orientation of single molecules, the optical operation of single switches at room temperature, excitonic interactions in a pair of single molecules, and the dynamics of excitons in a well-defined molecular system. We have no doubt that many of our current dreams will also materialize in the near future. For example, single emitters could become the basis of reliable and efficient sources of single photons. Single molecules and other emitting objects are ideal test benches for quantum manipulations because quantum effects are easier to produce and observe at molecular scales. Single nano-objects, such as molecules, can be used to probe the motion of charges in solid-state devices and conducting materials such as conjugated polymers. Other more established probes of dynamics in various materials at various conditions may also utilize single molecules. Much research in the fields of molecular biology and biophysics already benefits from the observations of single molecules or single nano-objects. Protein dynamics and folding as well as interactions between proteins, nucleic acids, and other biomolecules have already been demonstrated at the single-molecule level, and new exciting results can be expected. Single-molecule observations have surprised us not only by revealing unexpected and spectacular phenomena such as blinking, but also by displaying the full extent of heterogeneity in time and space at nanometer scales. These observations are also slowly changing the way we plan and interpret our experiments, opening a new field: nano-optics. And that is no minor achievement.

The *Annual Review of Physical Chemistry* is online at http://physchem.annualreviews.org

LITERATURE CITED

1. Moerner WE, Kador L. 1989. *Phys. Rev. Lett.* 62:2535–38
2. Orrit M, Bernard J. 1990. *Phys. Rev. Lett.* 65:2716–19
3. Güttler F, Irngartinger T, Plakhotnik T, Renn A, Wild UP. 1994. *Chem. Phys. Lett.* 217:393–97
4. Betzig E, Chichester RJ. 1993. *Science* 262:1422–25
5. Trautman JK, Macklin JJ, Brus LE, Betzig E. 1994. *Nature* 369:40–42
6. Ambrose WP, Goodwin PM, Martin JC, Keller RA. 1994. *Phys. Rev. Lett.* 72:160–63

7. Xie XS, Dunn RC. 1994. *Science* 265:361–64
8. Shera EB, Seitzinger NK, Davies LM, Keller RA, Soper SA. 1990. *Chem. Phys. Lett.* 174:553–57
9. Nie SM, Chiu DT, Zare RN. 1994. *Science* 266:1018–21
10. Trautman JK, Macklin JJ. 1996. *Chem. Phys.* 205:221–29
11. Macklin JJ, Trautman JK, Harris TD, Brus LE. 1996. *Science* 272:255–58
12. Lu HP, Xie XS. 1997. *Nature* 385:143–46
13. Xie XS. 1996. *Acc. Chem. Res.* 29:598–606
14. Funatsu T, Harada Y, Tokunaga M, Saito K, Yanagida T. 1995. *Nature* 374:555–59
15. Dickson RM, Norris DJ, Moerner WE. 1998. *Phys. Rev. Lett.* 81:5322–25
16. Plakhotnik T, Donley EA, Wild UP. 1997. *Annu. Rev. Phys. Chem.* 48:181–212
17. Xie XS, Trautman JK. 1998. *Annu. Rev. Phys. Chem.* 49:441–80
18. Deniz AA, Laurence TA, Dahan M, Chemla DS, Schultz PG, Weiss S. 2001. *Annu. Rev. Phys. Chem.* 52:233–57
19. Nie SM, Zare RN. 1997. *Annu. Rev. Biophys. Biomol. Struct.* 26:567–96
20. Basché T, Moerner WE, Orrit M, Wild UP, eds. 1997. *Single-Molecule Optical Detection, Imaging and Spectroscopy*. Weinheim, Ger.: Verlag Chem.
21. Zander C, Enderlein J, Keller RA, eds. 2002. *Single Molecule Detection in Solution*. Berlin: Wiley-VCH
22. Tamarat P, Maali A, Lounis B, Orrit M. 2000. *J. Phys. Chem. A* 104:1–16
23. Moerner WE. 2002. *J. Phys. Chem. B* 106:910–27
24. Kador L, Latychevskaia T, Renn A, Wild UP. 1999. *J. Chem. Phys.* 111:8755–58
25. Plakhotnik T, Palm V. 2001. *Phys. Rev. Lett.* 87:183602
26. Plakhotnik T. 2002. *J. Lumin.* 98:57–62

26a. Cohen-Tannoudji C, Diu B, Laloë F. 1977. *Quantum Mechanics*, p. 956. New York: Wiley; Paris: Hermann

27. Tokeshi M, Uchida M, Hibara A, Sawada T, Kitamori T. 2001. *Anal. Chem.* 73:2112–16
28. Boyer D, Tamarat P, Maali A, Lounis B, Orrit M. 2002. *Science* 297:1160–64

28a. Cognet L, Boyer D, Tamarat P, Lounis B. 2003. *Proc. Natl. Acad. Sci. USA* 100:11350–55

29. Tchénio P, Myers AB, Moerner WE. 1993. *J. Phys. Chem.* 97:2491–93
30. Myers AB, Tchénio P, Zgierski MZ, Moerner WE. 1994. *J. Phys. Chem.* 98:10377–90
31. Fleury L, Tamarat P, Lounis B, Bernard J, Orrit M. 1995. *Chem. Phys. Lett.* 236:87–95
32. Kummer S, Kulzer F, Kettner R, Basché T, Tietz C, et al. 1997. *J. Chem. Phys.* 107:7673–84
33. Bach H, Renn A, Wild UP. 2000. *Single Mol.* 1:73–77
34. Blum C, Stracke F, Becker S, Müllen K, Meixner AJ. 2001. *J. Phys. Chem. A* 105:6983–90
35. Christ T, Kulzer F, Bordat P, Basché T. 2001. *Angew. Chem. Int. Ed.* 40:4192–95
36. Jelezko F, Volkmer A, Popa I, Rebane KK, Wrachtrup J. 2003. *Phys. Rev. A* 67:041802
37. Nonn T, Plakhotnik T. 2001. *Chem. Phys. Lett.* 336:97–104
38. Plakhotnik T, Nonn T, Palm V. 2002. *Chem. Phys. Lett.* 357:397–402
39. Kiraz A, Ehrl M, Bräuchle C, Zumbusch A. 2003. *J. Chem. Phys.* 118:10821–23
40. Bobroff N. 1986. *Rev. Sci. Instrum.* 57:1152–57
41. Thompson RE, Larson DR, Webb WW. 2002. *Biophys. J.* 82:2775–83
42. Schmidt T, Schütz GJ, Baumgartner W, Gruber HJ, Schindler H. 1996. *Proc. Natl. Acad. Sci. USA* 93:2926–29
43. Kubitscheck U, Kückmann O, Kues T, Peters R. 2000. *Biophys. J.* 78:2170–79
44. Seisenberger G, Ried MU, Endreß T, Büning H, Hallek M, Bräuchle C. 2001. *Science* 294:1929–32
45. Yildiz A, Forkey JN, McKinney SA, Ha

T, Goldman YE, Selvin PR. 2003. *Science* 300:2061–65
46. Kao HP, Verkman AS. 1994. *Biophys. J.* 67:1291–1300
47. Dickson RM, Norris DJ, Tzeng YL, Moerner WE. 1996. *Science* 274:966–71
48. Magde D, Elson E, Webb WW. 1972. *Phys. Rev. Lett.* 29:705–8
49. Hess ST, Huang SH, Heikal AA, Webb WW. 2002. *Biochemistry* 41:697–705
50. Medina MA, Schwille P. 2002. *BioEssays* 24:758–64
51. Burns DH, Callis JB, Christian GD, Davidson ER. 1985. *Appl. Opt.* 24:154–61
52. Betzig E. 1995. *Opt. Lett.* 20:237–39
53. van Oijen AM, Köhler J, Schmidt J, Müller M, Brakenhoff GJ. 1998. *Chem. Phys. Lett.* 292:183–87
54. Bloeß A, Durand Y, Matsushita M, van der Meer H, Brakenhoff GJ, Schmidt J. 2002. *J. Microsc.* 205:76–85
55. Lacoste TD, Michalet X, Pinaud F, Chemla DS, Alivisatos AP, Weiss S. 2000. *Proc. Natl. Acad. Sci. USA* 97:9461–66
56. Güttler F, Sepioł J, Plakhotnik T, Mitterdorfer A, Renn A, Wild UP. 1993. *J. Lumin.* 56:29–38
57. Ha T, Laurence TA, Chemla DS, Weiss S. 1999. *J. Phys. Chem. B* 103:6839–50
58. Sepiol J, Jasny J, Keller J, Wild UP. 1997. *Chem. Phys. Lett.* 273:444–48
59. Fourkas JT. 2001. *Opt. Lett.* 26:211–13
60. Bartko AP, Dickson RM. 1999. *J. Phys. Chem. B* 103:3053–56
61. Forkey JN, Quinlan ME, Shaw MA, Corrie JET, Goldman YE. 2003. *Nature* 422:399–404
62. Vacha M, Kotani M. 2003. *J. Chem. Phys.* 118:5279–82
63. Sick B, Hecht B, Novotny L. 2000. *Phys. Rev. Lett.* 85:4482–85
64. Novotny L, Beversluis MR, Youngworth KS, Brown TG. 2001. *Phys. Rev. Lett.* 86:5251–54
65. Azoulay J, Debarre A, Jaffiol R, Tchenio P. 2001. *Single Mol.* 2:241–49
66. Debus C, Lieb MA, Drechsler A, Meixner AJ. 2003. *J. Microsc.* 210:203–8
67. Prummer M, Sick B, Hecht B, Wild UP. 2003. *J. Chem. Phys.* 118:9824–29
68. Empedocles SA, Neuhauser R, Bawendi MG. 1999. *Nature* 399:126–30
69. Chung IH, Shimizu KT, Bawendi MG. 2003. *Proc. Natl. Acad. Sci. USA* 100:405–8
70. Bernard J, Fleury L, Talon H, Orrit M. 1993. *J. Chem. Phys.* 98:850–59
71. Schenter GK, Lu HP, Xie XS. 1999. *J. Phys. Chem. A* 103:10477–88
72. Molski A. 2000. *Chem. Phys. Lett.* 324:301–6
73. Molski A, Hofkens J, Gensch T, Boens N, De Schryver F. 2000. *Chem. Phys. Lett.* 318:325–32
74. Verberk R, van Oijen AM, Orrit M. 2002. *Phys. Rev. B* 66:233202
75. Jung YJ, Barkai E, Silbey RJ. 2002. *J. Chem. Phys.* 117:10980–95
76. Yang H, Xie XS. 2002. *J. Chem. Phys.* 117:10965–79
77. Verberk R, Orrit M. 2003. *J. Chem. Phys.* 119:2214–22
78. Barsegov V, Mukamel S. 2002. *J. Chem. Phys.* 116:9802–10
79. Vlad MO, Moran F, Ross J. 2003. *Chem. Phys.* 287:83–90
80. Messin G, Hermier JP, Giacobino E, Desbiolles P, Dahan M. 2001. *Opt. Lett.* 26:1891–93
81. Kimble HJ, Dagenais M, Mandel L. 1977. *Phys. Rev. Lett.* 39:691–95
82. Diedrich F, Walther H. 1987. *Phys. Rev. Lett.* 58:203–6
83. Basché T, Moerner WE, Orrit M, Talon H. 1992. *Phys. Rev. Lett.* 69:1516–19
84. Brunel C, Lounis B, Tamarat P, Orrit M. 1999. *Phys. Rev. Lett.* 83:2722–25
85. Lounis B, Moerner WE. 2000. *Nature* 407:491–93
86. Beveratos A, Kuhn S, Brouri R, Gacoin T, Poizat JP, Grangier P. 2002. *Eur. Phys. J. D* 18:191–96
87. Treussart F, Alleaume R, Le Floc'h V,

Xiao LT, Courty JM, Roch JF. 2002. *Phys. Rev. Lett.* 89:093601
88. Zumbusch A, Fleury L, Brown R, Bernard J, Orrit M. 1993. *Phys. Rev. Lett.* 70:3584–87
89. Boiron AM, Tamarat P, Lounis B, Brown R, Orrit M. 1999. *Chem. Phys.* 247:119–32
90. Vainer YG, Naumov AV, Bauer M, Kador L. 2003. *Opt. Spectrosc.* 94:864–72
91. Vainer YG, Naumov AV, Bauer M, Kador L. 2003. *Opt. Spectrosc.* 94:873–84
92. Deschenes LA, Vanden Bout DA. 2001. *Science* 292:255–58
93. Vallée RAL, Tomczak N, Kuipers L, Vancso GJ, van Hulst NF. 2003. *Phys. Rev. Lett.* 91:038301
94. Caruge JM, Orrit M. 2001. *Phys. Rev. B* 64:205202–14
95. Basche T, Moerner WE. 1992. *Nature* 355:335–37
96. Basche T, Ambrose WP, Moerner WE. 1992. *J. Opt. Soc. Am. B* 9:829–36
97. Moerner WE, Plakhotnik T, Irngartinger T, Croci M, Palm V, Wild UP. 1994. *J. Phys. Chem.* 98:7382–89
98. Kummer S, Basché T, Bräuchle C. 1994. *Chem. Phys. Lett.* 229:309–16
98a. Kummer S, Basché T, Bräuchle C. 1994. *Chem. Phys. Lett.* 232:414
99. Kulzer F, Kummer S, Matzke R, Bräuchle C, Basché T. 1997. *Nature* 387:688–91
100. Kulzer F, Matzke R, Bräuchle C, Basché T. 1999. *J. Phys. Chem. A* 103:2408–11
101. Bordat P, Brown R. 2000. *Chem. Phys. Lett.* 331:439–45
102. Bordat P, Brown R. 2002. *J. Chem. Phys.* 116:229–36
103. Bordat P, Orrit M, Brown R, Würger A. 2000. *Chem. Phys.* 258:63–72
104. Dickson RM, Cubitt AB, Tsien RY, Moerner WE. 1997. *Nature* 388:355–58
105. Pierce DW, Hom-Booher N, Vale RD. 1997. *Nature* 388:338
106. Jung G, Wiehler J, Göhde W, Tittel J, Basché T, et al. 1998. *Bioimaging* 6:54–61
107. Garcia-Parajo MF, Segers-Nolten GMJ, Veerman JA, Greve J, van Hulst NF. 2000. *Proc. Natl. Acad. Sci. USA* 97:7237–42
108. Jung G, Bräuchle C, Zumbusch A. 2001. *J. Chem. Phys.* 114:3149–56
109. Jung G, Wiehler J, Steipe B, Bräuchle C, Zumbusch A. 2001. *Chem. Phys.* 2:392–96
110. Hugel T, Holland NB, Cattani A, Moroder L, Seitz M, Gaub HE. 2002. *Science* 296:1103–6
111. Irie M, Fukaminato T, Sasaki T, Tamai N, Kawai T. 2002. *Nature* 420:759–60
112. Ha T, Enderle T, Ogletree DF, Chemla DS, Selvin PR, Weiss S. 1996. *Proc. Natl. Acad. Sci. USA* 93:6264–68
113. Zhuang XW, Ha T, Kim HD, Centner T, Labeit S, Chu S. 2000. *Proc. Natl. Acad. Sci. USA* 97:14241–44
114. Tinnefeld P, Weston KD, Vosch T, Cotlet M, Weil T, et al. 2002. *J. Am. Chem. Soc.* 124:14310–11
115. Hofkens J, Schroeyers W, Loos D, Cotlet M, Köhn F, et al. 2001. *Spectrochim. Acta A* 57:2093–107
116. Hettich C, Schmitt C, Zitzmann J, Kühn S, Gerhardt I, Sandoghdar V. 2002. *Science* 298:385–89
117. McDermott G, Prince SM, Freer AA, Hawthornthwaite-Lawless AM, Papiz MZ, et al. 1995. *Nature* 374:517–21
118. Bopp MA, Jia YW, Li LQ, Cogdell RJ, Hochstrasser RM. 1997. *Proc. Natl. Acad. Sci. USA* 94:10630–35
119. Bopp MA, Sytnik A, Howard TD, Cogdell RJ, Hochstrasser RM. 1999. *Proc. Natl. Acad. Sci. USA* 96:11271–76
120. van Oijen AM, Ketelaars M, Köhler J, Aartsma TJ, Schmidt J. 2000. *Biophys. J.* 78:1570–77
121. van Oijen AM, Ketelaars M, Köhler J, Aartsma TJ, Schmidt J. 1999. *Science* 285:400–2
122. Ketelaars M, van Oijen AM, Matsushita M, Köhler J, Schmidt J, Aartsma TJ. 2001. *Biophys. J.* 80:1591–603
123. Tietz C, Chekhlov O, Dräbenstedt A, Schuster J, Wrachtrup J. 1999. *J. Phys. Chem. B* 103:6328–33

124. Hofmann C, Ketelaars M, Matsushita M, Michel H, Aartsma TJ, Köhler J. 2003. *Phys. Rev. Lett.* 90:013004
125. Gerken U, Wolf-Klein H, Huschenbett C, Götze B, Schuler S, et al. 2002. *Single Mol.* 3:183–88
126. Gerken U, Jelezko F, Götze B, Branschädel M, Tietz C, et al. 2003. *J. Phys. Chem. B* 107:338–43
127. Jelezko F, Tietz C, Gerken U, Wrachtrup J, Bittl R. 2000. *J. Phys. Chem. B* 104:8093–96
128. Zehetmayer P, Hellerer T, Parbel A, Scheer H, Zumbusch A. 2002. *Biophys. J.* 83:407–15
129. Wu M, Goodwin PM, Ambrose WP, Keller RA. 1996. *J. Phys. Chem.* 100:17406–9
130. Dunn RC, Allen EV, Joyce SA, Anderson GA, Xie XS. 1995. *Ultramicroscopy* 57:113–17
131. Ying LM, Xie XS. 1998. *J. Phys. Chem. B* 102:10399–409
132. Gensch T, Hofkens J, Heirmann A, Tsuda K, Verheijen W, et al. 1999. *Angew. Chem. Int. Ed.* 38:3752–56
133. Hofkens J, Maus M, Gensch T, Vosch T, Cotlet M, et al. 2000. *J. Am. Chem. Soc.* 122:9278–88
134. Gronheid R, Hofkens J, Köhn F, Weil T, Reuther E, et al. 2002. *J. Am. Chem. Soc.* 124:2418–19
135. Christ T, Kulzer F, Weil T, Müllen K, Basché T. 2003. *Chem. Phys. Lett.* 372:878–85
136. Vanden Bout DA, Yip WT, Hu DH, Fu DK, Swager TM, Barbara PF. 1997. *Science* 277:1074–77
137. Yip WT, Hu DH, Yu J, Vanden Bout DA, Barbara PF. 1998. *J. Phys. Chem. A* 102:7564–75
138. Hu DH, Yu J, Barbara PF. 1999. *J. Am. Chem. Soc.* 121:6936–37
139. Hu DH, Yu J, Wong K, Bagchi B, Rossky PJ, Barbara PF. 2000. *Nature* 405:1030–34
140. Yu J, Hu DH, Barbara PF. 2000. *Science* 289:1327–30

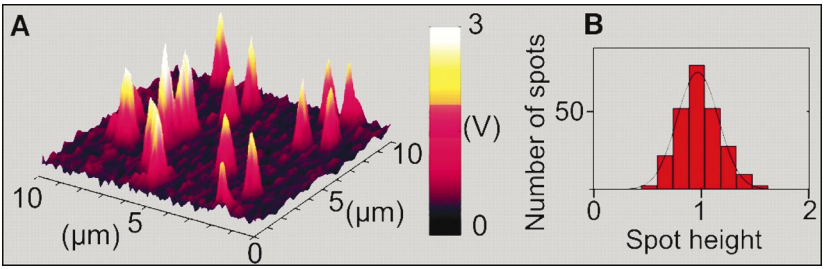

Figure 1 (*A*) Photothermal images of 5-nm gold particles in a few tens-of-nanometers-thick polyvinyl alcohol film on a glass substrate. The average heating power was 20 mW. The image was obtained in 100 s with a modulation frequency of 800 kHz and an integration time of 10 ms per pixel. The high S/N and the relatively narrow distribution of spot intensities are apparent. (*B*) Histogram of spot maximum intensities. The fairly narrow and monomodal distribution confirms that the spots correspond to single nanoparticles. Reprinted with permission from Boyer et al. (28). Copyright 2002, American Association for the Advancement of Science.

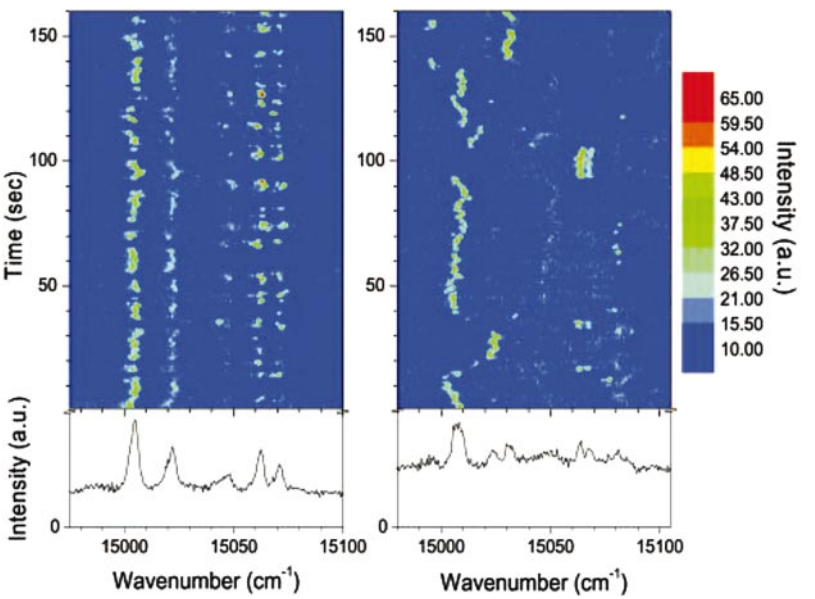

Figure 2 High-resolution and lange-bandwidth emission spectra of two terrylenediimide (TDI) molecules in a PMMA host. Excitation is at 16498 cm^{-1} with a few mW. Reprinted with permission from Kiraz et al. (39). Copyright 2003, American Institute of Physics.

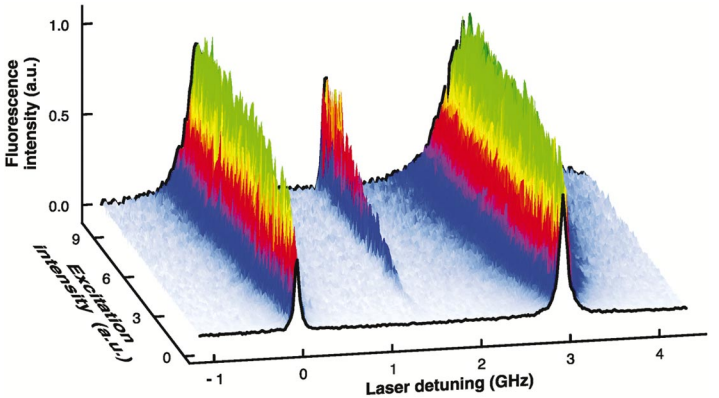

Figure 5 Background-corrected excitation spectra of two coupled terrylene molecules for a wide range of laser intensities. The new line at high intensities arises from simultaneous excitation of both molecules. Reprinted with permission from (116). Copyright 2002 American Association for the Advancement of Science.

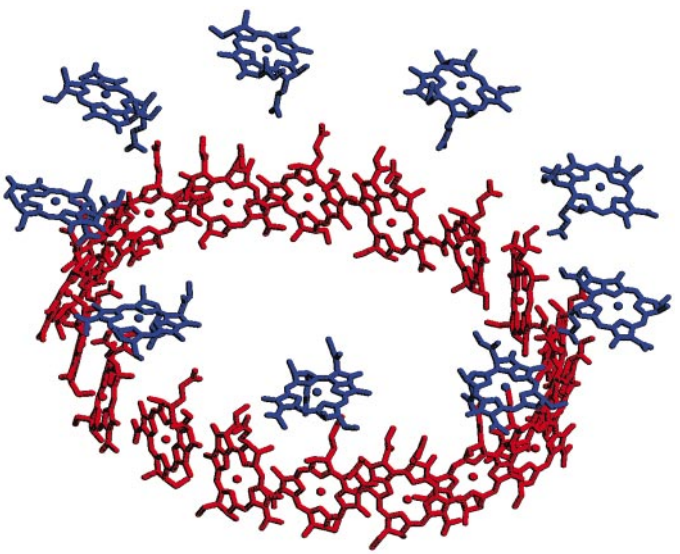

Figure 6 The schematic representation of the arrangement of the 27 BChl a chromophores in the LH2 complex of *Rhodopseudomonas acidophila,* as determined from an X-ray structure (117). The B800 ring (*blue*) consists of 9 BChl a molecules in an arrangement with a ninefold symmetry axis that coincides with the overall axis of the cylindrical complex; the individual pigments are well separated with their molecular planes perpendicular to the C_9 axis. The 18 chromophores of the B850 ring (*red*), on the other hand, are spaced more closely with their planes roughly parallel to the common C_9 axis, somewhat similar to the arrangement of the blades around the axle of a turbine. This figure was created from the Protein Data Bank record 1KZU.

Annual Review of Physical Chemistry
Volume 55, 2004

CONTENTS